

Supplementary Information

Highly efficient field emission properties of radially aligned carbon nanotubes

Prashant Tripathi^a, Bipin Kumar Gupta^b, Ashish Bhatnagar^a, C. R. P. Patel^a, Prashant K. Banker^c, Dattatray J. Late^c, Mahendra A. More^d, N. P. Lalla^c, D. M. Phase^c, R. J. Choudhary^c, M. A. Shaz^a, P. M. Ajayan^{f,*}, and O. N. Srivastava^{a,*}

^a Nano Science Unit, Department of Physics, Institute of Science, Banaras Hindu University, Varanasi - 221005, India

^b CSIR- National Physical Laboratory, New Delhi -110012, India.

^c Physical and Materials Chemistry Division, CSIR-National Chemical Laboratory, Dr. Homi Bhabha Road, Pashan, Pune - 411008, India.

^d Department of Physics, Savitribai Phule Pune University, Pune - 411007, India.

^e UGC-DAE Consortium for Scientific Research, Khandwa Road, Indore, Madhya Pradesh -452001, India.

^f Department of Materials Science and Nano Engineering, Rice University, Houston, Texas -77005, USA.

*Email: heponsphy@gmail.com, ajayan@rice.edu.

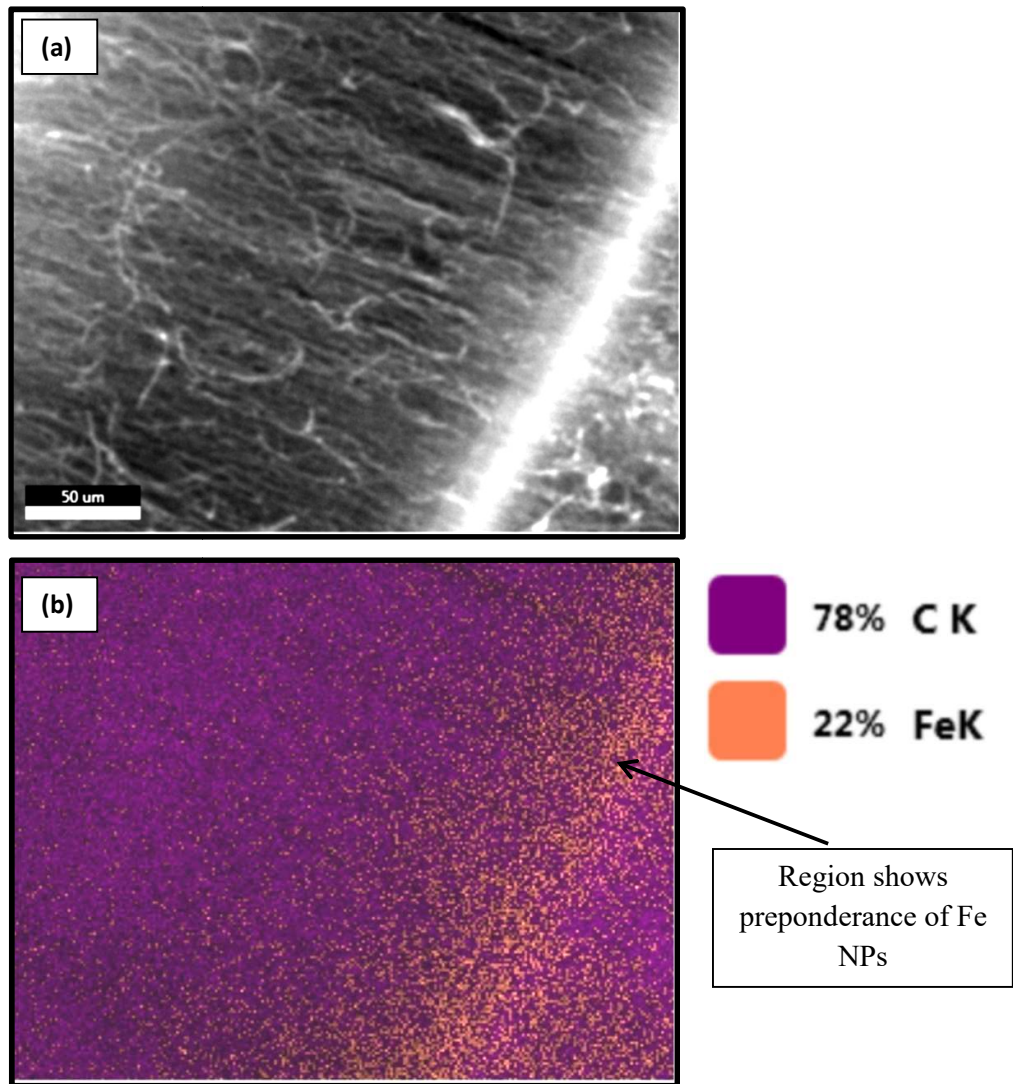


Fig. S1a) SEM micrograph of a segment of CHC 85/20 and corresponding EDX mapping image b). Bright part in a) is showing the region between two stacks of radially aligned CNTs and corresponding EDX mapping image is showing that Fe NPs (shown by yellow colour) are present almost everywhere but have preponderance in between two stacks.

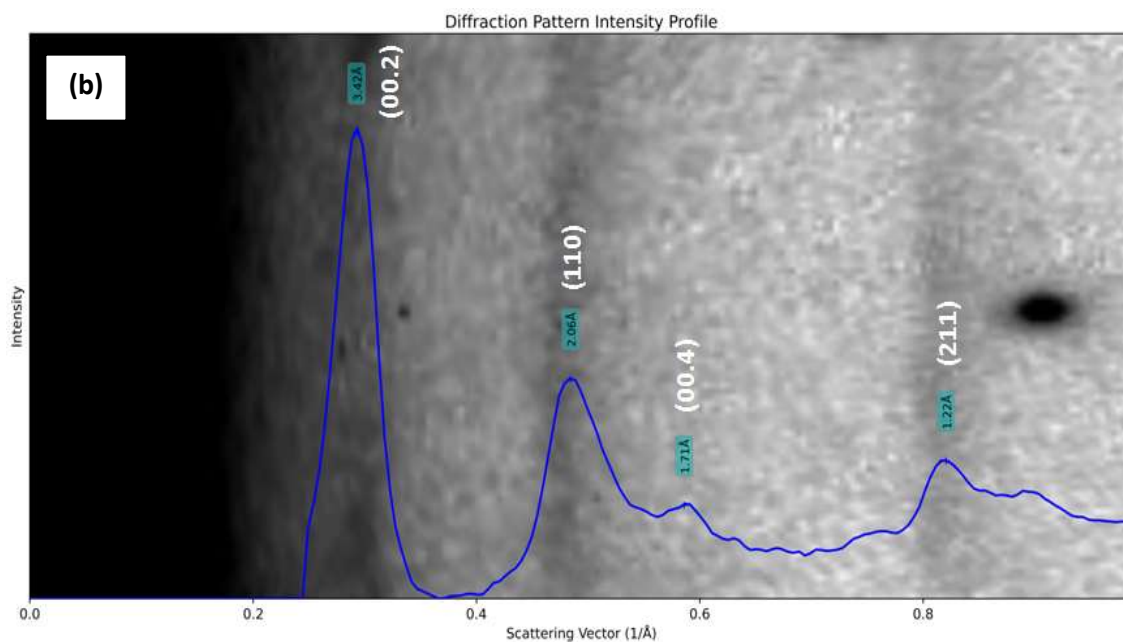
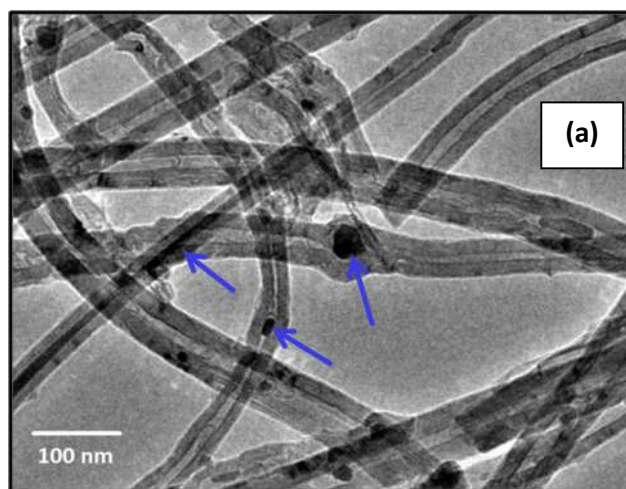


Fig. S2 Typical TEM micrograph (Fig. S2a) of carbon nanotubes confirm the presence of Fe NPs in between the nanotubes (blue arrows show the presence of Fe NPs), b) Diffraction pattern intensity profile of SAD pattern of Fig. 2 g) using diffraction_ring_profiler_software.

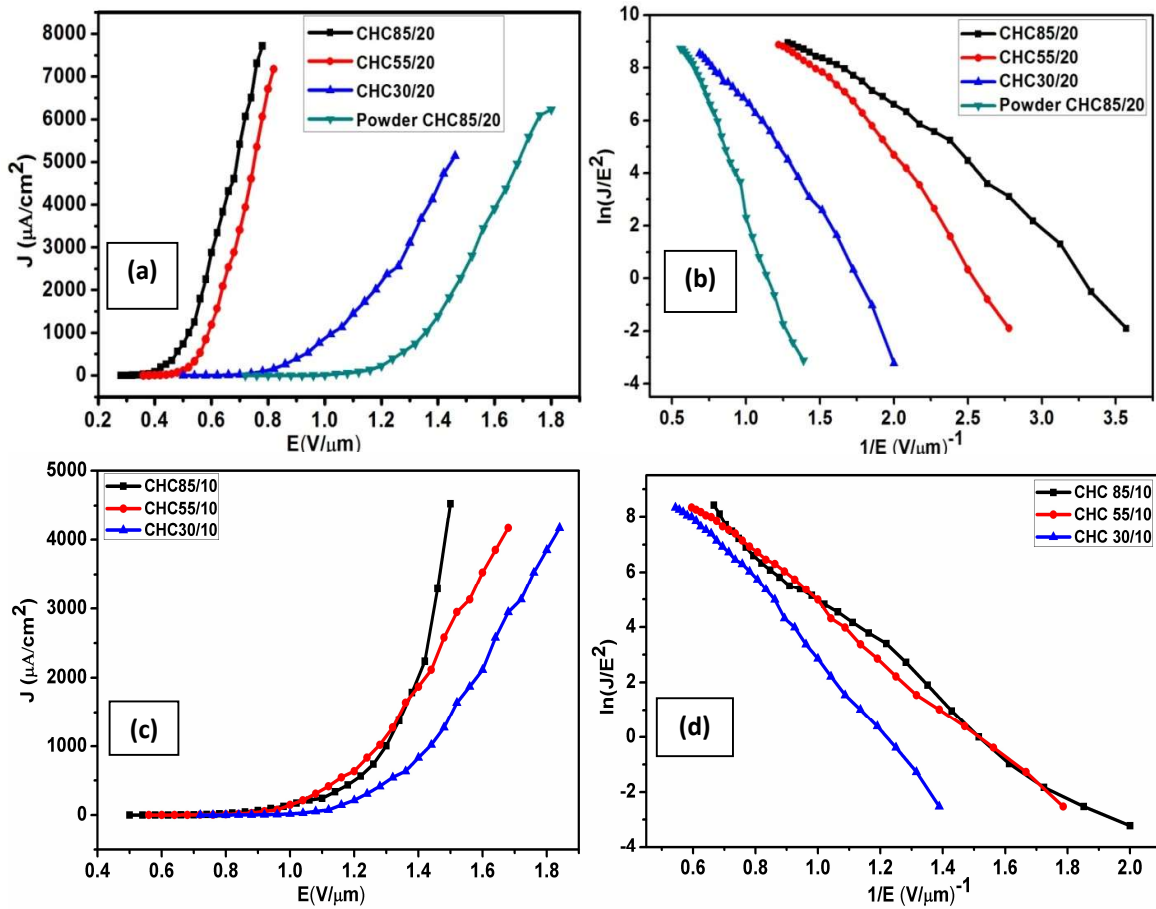


Fig. S3 Comparative field emission characteristics, a) and c) current density (J) as a function of applied electric field (E), b) and d) F-N plot $\{ \ln(J/E^2) \text{ versus } 1/E \}$, of CHC 85/20, powder CHC 85/20, CHC 85/10, CHC 55/20, CHC 55/10, CHC 30/20, CHC 30/10, respectively.

S(A): In order to investigate the role of alignment of CNTs inside CHCs, we crushed the cylinder made from CHC85/20 into powder form and mounted it as cathode and performed field emission experiment. We have found that the turn on and threshold field shifted to $1.00 \text{ V}/\mu\text{m}$ and $1.14 \text{ V}/\mu\text{m}$ from 0.35 and $0.41 \text{ V}/\mu\text{m}$, respectively. The maximum current density for crushed cylinder decreases from 7.71 to $6.23 \text{ mA}/\text{cm}^2$ and corresponding applied field increases from 0.78 to $1.80 \text{ V}/\mu\text{m}$. The change in the field emission characteristics values are due to breaking of the highly ordered alignment of the tubes of the CHC into small bundles. To check the role of stacked nature of CNTs of the cylinder, we have reduced the thickness of the CHC. It has been found that the field emission performance deteriorated on reducing the number of stacks. Moreover, the experiment was run for 4 cycles to check the reliability of the result (Fig. S5). The whole field emission measurement data are summarised in Figs S3, S4 and table S1. These results confirm that the cylinders with diameter of 20 mm show better

field emission performances as compared to 10 mm. These results also show that the field emission properties are concentration and diameter dependent (summarised in table S1). Hence, the field emission properties can be tuned by varying the concentration and diameter of the CHCs.

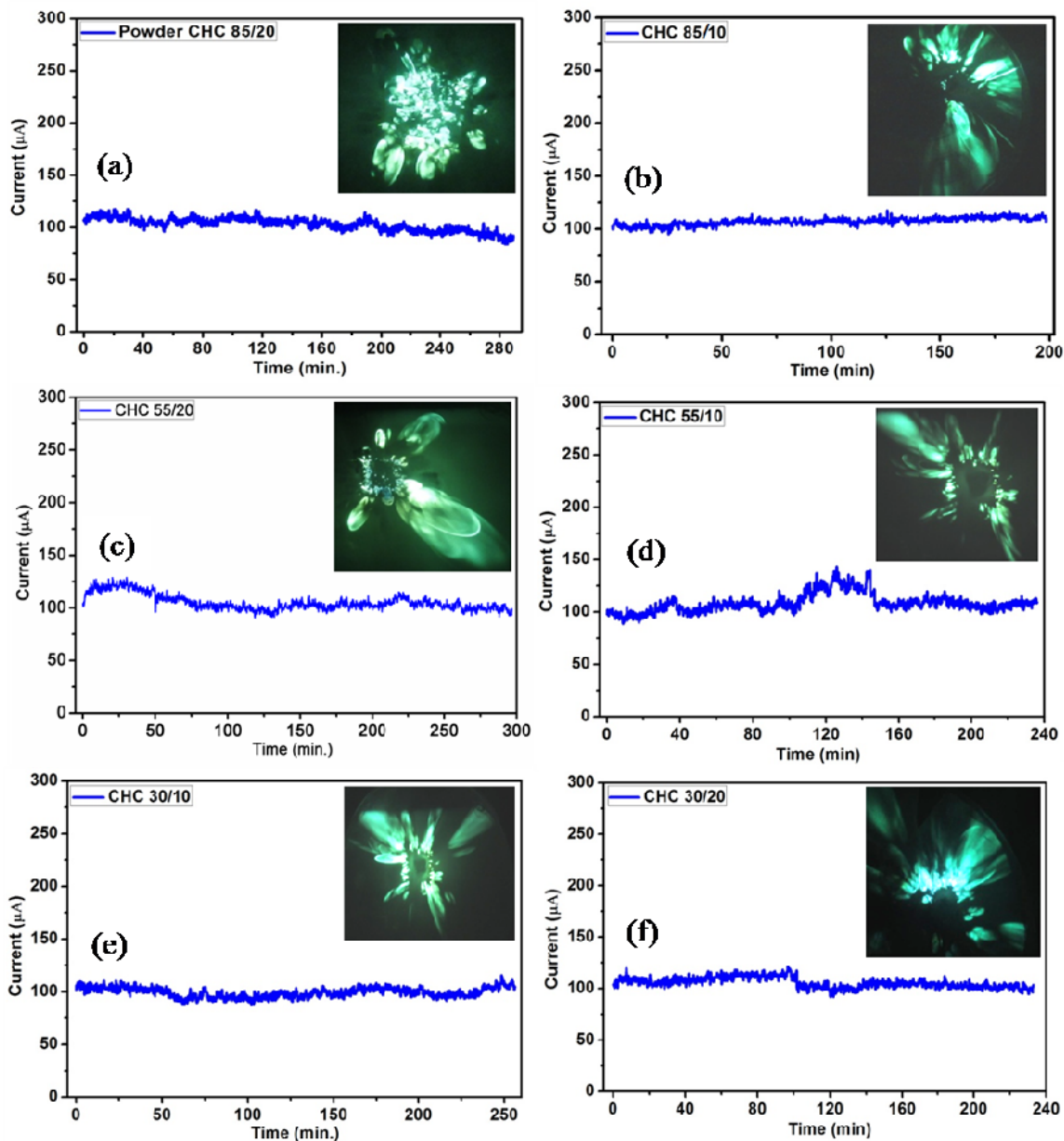


Fig. S4 Field emission current stability (i-t) plots and corresponding field emission images (inset); of a) powder CHC 85/20, b) CHC 85/10, c) CHC 55/20, d) CHC 55/10, e) CHC 30/20 and f) CHC 30/10, respectively.

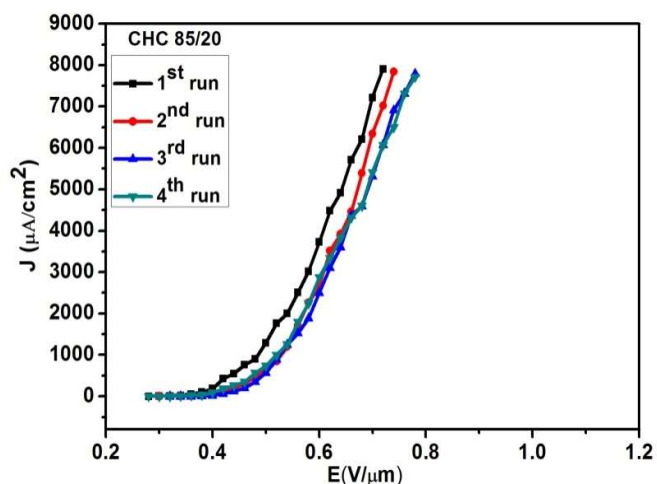


Fig. S5 Current density (J) versus E plots of CHC 85/20 from 1st to 4th cycle run, showing better emission stability.

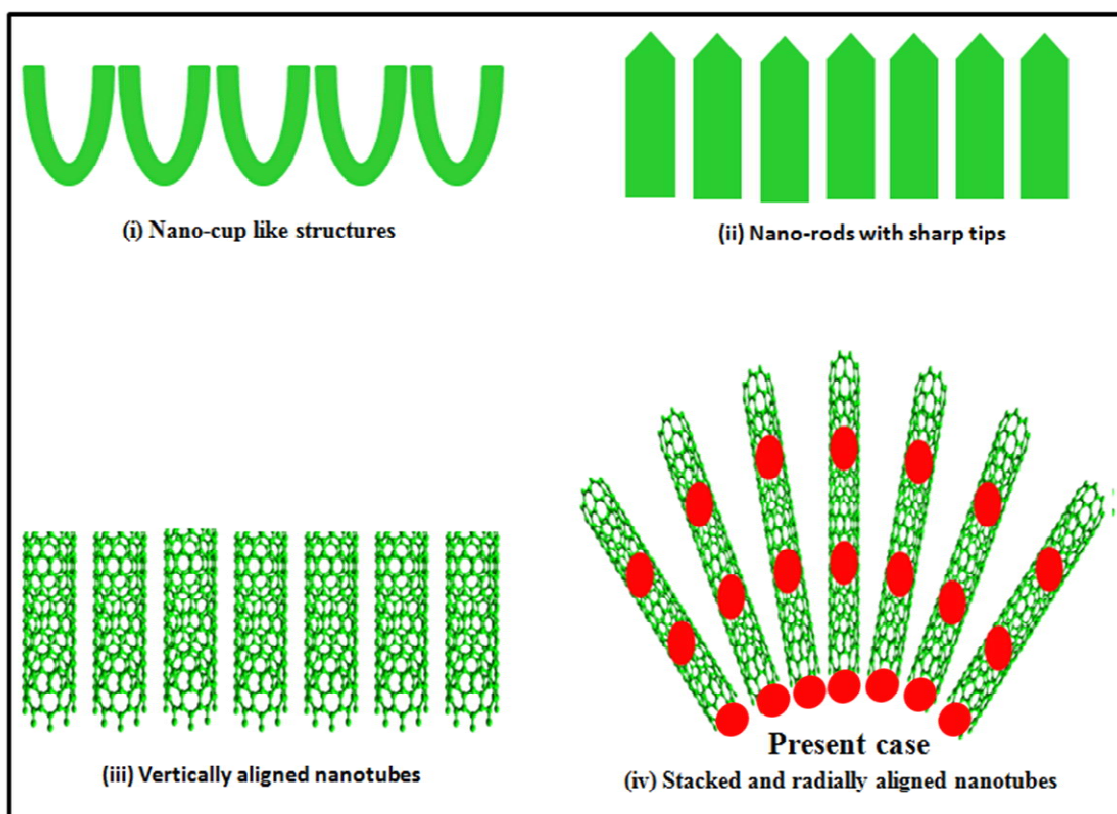


Fig. S6 Schematic of the possible configuration for the field emission using different structures.

S(B): The present structure (carbon hollow cylinder) shows better field emission properties than others (Fig. S6). The demerits of above three structures can be understood as follow. In nano-cup like structure, turn on field can be tailored / lowered by reducing the screening

effect i.e. increasing the distance between nano-cups but at the same time, current density decreases due to insufficient number of emitter sites.¹ The problems with the nano-rod type of structures are that due to large screening effect between the rods, turn on and threshold field was very large. Some efforts were done to improve the turn on and threshold field by reducing the tip size of the rods; it was found that the turn on and threshold field were improved but this was not sufficient since screening effect was dominant between rods/tubes.^{2,3} The third type of structure also suffers from high screening effect because of the small separation between the tubes. However, some work showed reducing the screening effect by increasing the separation between the tubes but enhancement in current density was not sufficient.⁴⁻⁶

S. No.	Sample	Slope (m)	β - factor	Turn on field at 10 $\mu\text{A}/\text{cm}^2$	Threshold field at 100 $\mu\text{A}/\text{cm}^2$	J_{max}
1	CHC 85/20	-4.52	1.34×10^4	0.35 V/ μm	0.41 V/ μm	7.71 mA/cm ² at 0.78 V/ μm
2	Powder CHC 85/20	-15.41	0.48×10^4	1.00 V/ μm	1.14 V/ μm	6.23 mA/cm ² at 1.80 V/ μm
3	CHC 85/10	-9.06	0.69×10^4	0.76 V/ μm	0.96 V/ μm	4.52 mA/cm ² at 1.50 V/ μm
4	CHC 55/20	-6.89	1.08×10^4	0.43 V/ μm	0.49 V/ μm	7.17 mA/cm ² at 0.82 V/ μm
5	CHC 55/10	-9.36	0.80×10^4	0.82 V/ μm	0.98 V/ μm	4.16 mA/cm ² at 1.68 V/ μm
6	CHC 30/20	-8.32	0.89×10^4	0.64 V/ μm	0.80 V/ μm	5.14 mA/cm ² at 1.46 V/ μm
7	CHC 30/10	-9.46	0.79×10^4	0.74 V/ μm	0.94 V/ μm	3.42 mA/cm ² at 1.56 V/ μm

Table S1. Field emission measurements of CHC 85/20, powder CHC 85/20, CHC 85/10, CHC 55/20, CHC 55/10, CHC 30/20, CHC 30/10 { β factor calculations for CHC 85/20 was done by taking work function values 4.3 eV, the rest calculations (powder CHC 85/20, CHC 85/10, CHC 55/20, CHC 55/10, CHC 30/20, CHC 30/10) were done by assuming the work function value of 4.95 eV }.

S. No.	Material (References from main manuscript)	Turn ON Voltage	Jmax at applied voltage	Field enhancement Factor	Synthesis procedure
1.	Hafnium oxide coated carbon nanotubes (Ref. 26)	2 V/ μ m	0.12 mA/cm ² at 5 V/ μ m	-----	Atomic layer chemical vapor deposition was employed for coating the CNT emitter with hafnium oxide
3.	Millimeter long CNTs (Ref. 11)	0.17 V/ μ m	750 mA/cm ² at 0.45 V/ μ m	3.2x 10 ⁴	Millimetre long CNTs were prepared by floating catalyst CVD process. Si substrate were patterned with a photo resin mask and covered with 50 nm thick gold film deposited by DC sputtering.
2.	Carbon nanotube yarn formed on carpet (Ref. 10)	0.33 V/ μ m	~17 mA/cm ² at 0.6 V/ μ m	1.9 x 10 ⁴	Synthesis of CNT yarn by direct spinning through CVD & then CNT yarns were tied to a conductive substrate using a knot and cut by hand
1.	CNT Arrays Synthesized on Inconel Super alloy (Ref. 9)	~ 1.5 V/ μ m	~ 100 mA/cm ² at > 4 V/ μ m	~ 7.3x 10 ³	Vertically aligned MWCNTs were synthesized using a water assisted CVD process on Si & Inconel substrate coated with 10 nm Al buffer & 1.5 nm Fe catalyst layer using e-beam evaporation technique
4.	Metal decorated carbon nanotubes (Ref. 20)	0.13 V/ μ m	840 μ A/cm ² at 0.15 V/ μ m	-----	CNTs were grown on Al coated Si/inconel and then the grown CNTs were kept inside the CVD chamber with Al sheet over them and heated upto 700°C for 10 min and cooled gradually
6.	Carbon nanotube field emitters after high temperature thermal annealing (Ref. 27)	1.15 V/ μ m,	8.5 A/cm ² at 4.6 V/ μ m.	2233	The carbon nanotube (CNT) field emitters have been fabricated by attaching a CNT film on a graphite rod using graphite adhesive material and then annealed at high temperature (900°C) in vacuum ambient.

8.	carbon nanotube line emitters fabricated using mechanical clamping process (Ref. 28)	4.8 V/ μm	2700 mA/cm ²	-----	To prepare the growth substrate, an 18 nm thick aluminum (Al)-barrier layer was deposited on a (100) silicon (Si) wafer by electron beam (e-beam) evaporation. 1.0 nm thick iron (Fe) thin film as a catalyst for CNT growth is deposited by e-beam deposition over the Si substrate. CNT line emitters were fabricated by using macroscopic mechanical clamping process.
9.	CHC 85/20 (Present Case)	0.35 V/ μm	7.71 mA/cm ² at 0.78 V/ μm	1.34 x 10 ⁴	Fe bearing multi stacked radially aligned CNTs based CHC was prepared by CVD method (one pot and easy to synthesize in bulk)

Table S2. Comparative study of the present work with other important works reported in literature.

References:

1. Gupta BK, Kedawat G, Kumar P, Singh S, Suryawanshi SR, Agrawal (Garg) N et al. Field emission properties of highly ordered low-aspect ratio carbon nano-cup arrays. RSC Adv2016; 6: 9932.
2. Pan N, Xue H, Yu M, Cui X, Wang X, Hou JG et al. Tip-morphology-dependent field emission from ZnO nanorod arrays. Nanotechnology2010;21:225707.
3. Chen HW, Yang HW, He HM, Lee YM. ZnO nanorod arrays prepared by chemical bath deposition combined with rapid thermal annealing: structural, photoluminescence and field emission characteristics. J. Phys. D: Appl. Phys.2016;49:025306.
4. Nilsson L, Groening O, Emmenegger C, Kuettel O, Schaller E, Schlapbach L et al. Scanning Field Emission from Patterned Carbon Nanotube Films. Appl. Phys. Lett.2000;76:2071.
5. Bonard JM, Dean KA, Coll BF. Field Emission of Individual Carbon Nanotubes in the Scanning Electron Microscope. Phys. Rev. Lett.2002; 89:197602.
6. Bonard JM, Weiss N, Kind H, Stöckli T, Forró L, Kern K et al. Tuning the Field Emission Properties of Patterned Carbon Nanotube Films. Adv. Mater. 2001;13:84.